



Seismic wave propagation to diagnose the state of fracturing

by M.W. Hildyard*, R.P. Young†, D.S. Collins‡, and W. Pettitt§

Synopsis

The aim of this paper is to demonstrate that active seismic measurements could have an impact in helping solve rock engineering problems experienced in the South African mining industry. The paper presents a variety of experimental and numerical results where seismic waves show clear differences in wave-speed and amplitudes due to different degrees of fracturing. It presents results from the 'Omnibus' project commissioned to develop new ultrasonic technologies for diagnosing fracturing for nuclear waste repositories. This included using models to investigate assemblies of cracks where the effects of crack density and crack size on waveforms are shown to be coupled. Results indicate that these effects can be decoupled in the frequency domain, where the Fourier amplitude aids in estimating crack size, while the low frequency phase-difference has a direct relationship to crack density. Models are also shown to aid interpretation of waveforms by isolating geometric effects from the effects due to cracks. Two rock engineering problems experienced in the South African mining industry are investigated through numerical examples. These demonstrate that determining whether 'crush' pillars have failed and determining the degree of fracturing in the hangingwall of stopes, may be possible through the use of active seismic surveys.

Introduction

The purpose of this paper is to demonstrate that active seismic measurements can aid the interpretation of the fracturing and jointing in rock, and hence could be of significant benefit to rock engineering problems on South African mines. The paper covers the theory, applications in other engineering fields, and numerical examples of how these methods could be applied to pillar problems and hangingwall problems in South African mines.

It is well known in seismology that fracturing in the rock leads to both attenuation and slowing of seismic waves (e.g. O'Connell and Budiansky, 1974; Crampin, 1981; Hudson, 1981; Gibowicz and Kijko, 1994). These properties are in fact the physical principles by which both active and passive seismic tomography methods have been developed for analysing the rockmass (e.g. Young and Maxwell, 1992; Maxwell and

Young, 1996). Maxwell and Young (1996) include a case study of a tomography performed on a stability pillar in South Africa at the Blyvooruitzicht mine.

Recent years have seen the development of ultrasonic methods for monitoring fracturing in rock (e.g. Carlson and Young, 1993; Collins, 1997; Young and Collins, 2001; Pettitt *et al.*, 2001). Ultrasonic technology involves the use of high frequency (> 30 kHz) transducers as transmitters or receivers of elastic waves. The development of these methods has been significantly driven by the need to investigate the feasibility of deep geological disposal of nuclear waste. One of the challenges for safe disposal is to establish the integrity of the 'rock barrier' over long periods of time, possibly tens of thousands of years. Monitoring tools are therefore being developed to aid this evaluation in field experiments conducted at large-scale underground research facilities. Active ultrasonic surveys use electrically activated transducers to transmit seismic waves through the rock to an array of receivers. The transmission of these waves is influenced by the density, size and orientation of fractures, state of stress and fluid content. The surveys therefore provide a non-invasive means of measuring the internal structure of the rock.

Figure 1 shows an example of ultrasonic waveforms recorded in a laboratory experiment on triaxially loaded sandstone cubes (Baker and Pettitt, 2003). This experiment formed part of the 'Omnibus' project. The figure shows waveforms during a cycle of hydrostatic loading of 5, 10, 20, 40,

* CSIR Division of Mining Technology, Auckland Park, South Africa.

† Lasonde Institute, University of Toronto, Canada.

‡ Department of Earth Sciences, University of Liverpool, UK.

§ Applied Seismology Consultants (ASC), UK

© The South African Institute of Mining and Metallurgy, 2005. SA ISSN 0038-223X/3.00 + 0.00. Paper received Apr. 2005; revised paper received Jun. 2005.

Seismic wave propagation to diagnose the state of fracturing

60, 80 and 100 MPa. It can clearly be seen that the arrival times decrease and hence the wave-speed increases considerably during the loading. The amplitudes were similarly increased. The experiment used true triaxial loading to generate cracking along a single direction. Figure 1b compares waveforms prior to and after the generation of new cracks, and the induced cracking leads to a significant delay in the arrival and a ten-fold decrease in amplitude.

Although there are often demonstrable differences in the recorded ultrasonic waveforms, the interpretation of fracturing from the waveforms is not well established. This paper therefore focuses on how coupling numerical modelling with these surveys can improve the interpretation of fracturing. Hildyard (2001) successfully used this approach in interpreting waveforms from an ultrasonic survey at the Underground Research Laboratory (URL) in Canada. Results from the ultrasonic survey (Carlson and Young, 1992) showed significant differences between paths parallel to and paths oblique to the tunnel surface. Figure 2 shows a

comparison of waveforms from a purely elastic model with the ultrasonic waveforms collected during this field experiment, clearly showing the reduced wave-speed and the increased attenuation for paths oblique to the tunnel surface. Through the use of fracture models, Hildyard (2001) was able to provide insight into the density, size and orientation of fracturing causing this behaviour.

The modelling results in this paper were obtained using the program WAVE (Cundall, 1992; Hildyard *et al.*, 1995). This is a code developed for analysing the interaction of seismic waves with underground openings and with fractures in rock. It uses a fourth order accurate, staggered-grid finite difference scheme. Zero-width cracks are modelled by implementing explicit boundary conditions on the crack surfaces. In this paper all cracks are open, although more complex crack conditions can be modelled. Detail on the grid scheme and on the implementation of cracks can be found in Hildyard (2001).

The paper shows that explicit modelling of wave

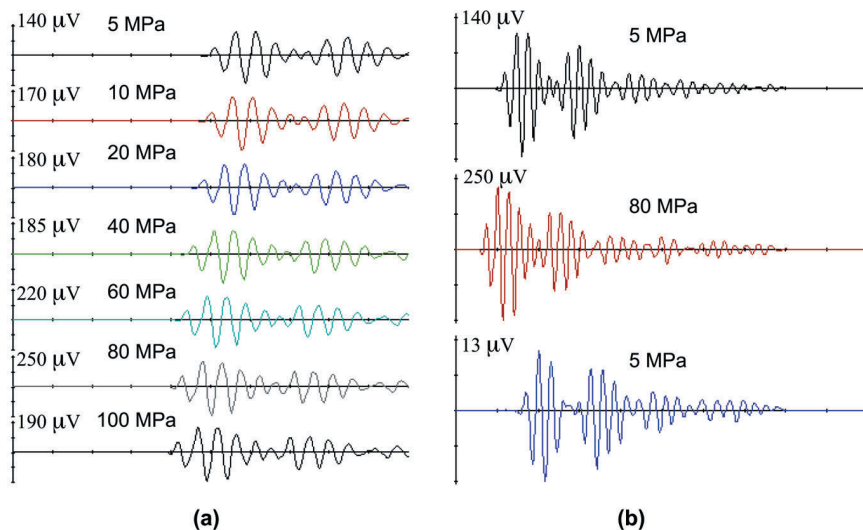


Figure 1—Example waveforms from the laboratory sandstone experiments at different stages during a hydrostatic loading cycle: (a) cycle of increasing stress from 5 MPa through to 100 MPa (b) stages of 5 MPa and 80 MPa load (pre-crack generation) and 5 MPa load (after the generation of new cracks)

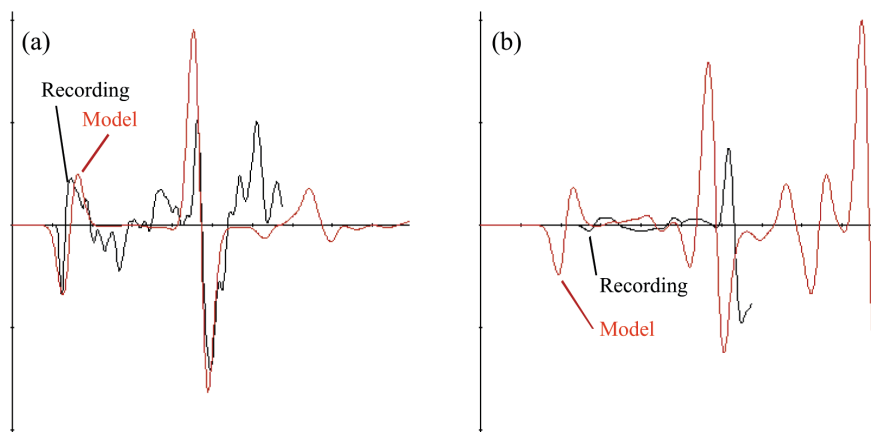


Figure 2 Traces for two of the recorded seismograms in an ultrasonic experiment by Carlson and Young (1993), compared to those simulated using an elastic model. The comparison in (a) is typical for source-receiver paths, which were approximately parallel to the tunnel surface, while the comparison in (b) is typical for source-receiver paths oblique to the tunnel surface

Seismic wave propagation to diagnose the state of fracturing

interaction with fracturing can improve the interpretation of fracturing in seismic measurements, helping quantify fracture density, size and orientation. It presents a frequency-domain method for analysing changes in wave-speed and attenuation. It then covers a European Union funded project ('Omnibus') where these models were used in the development of more advanced interpretation software. Finally, the paper demonstrates through the use of simple numerical examples that such technology could be of benefit in addressing rock engineering problems experienced in mining. Seismic velocity surveys are not widely conducted in the South African mining industry to study rock fractures. Through current parliamentary-funded projects, CSIR-Miningtek is taking the initial steps to evaluate the use and benefits of active seismic velocity surveys in the South African mining industry.

The effect of assemblies of cracks on wave-speed and attenuation

One conceptual model of fracturing is a collection of flat openings. O'Connell and Budiansky (1974) used energy considerations to develop a dimensionless quantity describing the relative effect of a collection of cracks. This crack density is defined as

$$\varepsilon = (2N / \pi) \langle A^2 / P \rangle \quad [1]$$

where brackets denote an average, A the crack area, P the crack perimeter and N the number of cracks per unit volume. For circular cracks, the crack density is simply proportional to the cube of the crack radius a :

$$\varepsilon = \frac{1}{V} \sum a^3 \quad [2]$$

A methodology was developed in a recent doctoral thesis (Hildyard, 2001) whereby wave-speed and attenuation spectra can be derived for a simulated cracked sample with a known crack density by passing a plane wave through it. The results are the average results for all parallel paths through the cracked samples. The simulation of a plane wave has the major advantage that the results are independent of any geometrical effects.

The method involves creating a model with a simulated crack geometry such as the random assembly as shown in Figure 3, passing a plane wave through the model, and recording the received waveform at some distance through the sample. Waveforms are averaged across a receiving plane to obtain an average effect. The Fourier phase and Fourier amplitude spectra of these waveforms are then compared with a waveform recorded in a perfect elastic medium at a position at the start of the cracked region. The effect of the cracked sample on amplitude and phase velocity can be obtained as a function of frequency using

$$c = c(\omega) \approx \frac{-\omega(x_2 - x_1)}{(\phi_2 - \phi_1)} \quad [3]$$

$$A(\omega) = \left(\frac{A_2}{A_1} \right)^{\frac{L}{x_2 - x_1}} \quad [4]$$

where $c(\omega)$ is the phase velocity, $\phi_1(\omega)$ and $A_1(\omega)$ are the Fourier phase and amplitude functions of the waveform recorded at position x_1 for an elastic medium, $\phi_2(\omega)$ and $A_2(\omega)$ are the Fourier phase and amplitude functions of the waveform recorded at position x_2 , for the cracked medium and L is a selected unit length of interest.

Figure 4a shows an example of the effect of different crack densities on time-domain waveforms. Figures 4b and 4c show the effects in the Fourier domain for amplitude and phase angle. Applying Equations [3] and [4] yields the phase velocity and the attenuation spectra for the crack assembly as shown in Figure 5. Significantly, the time domain waveforms do not show a clear difference in arrival time (Figure 4a)—while the calculated phase velocity in Figure 5, clearly indicates a reduction in velocity for the low frequency region. The wave-speed is slowed for low frequencies, whilst attenuation dominates at high frequencies. The frequency at which this transition occurs depends upon the crack sizes. During this transition the wave-speed is not constant but decreases from its low-frequency value, until for high frequency and high attenuation it returns to the elastic wave-speed. The full method, some of the issues about its usage, and further P-wave results are covered in Hildyard (2001).

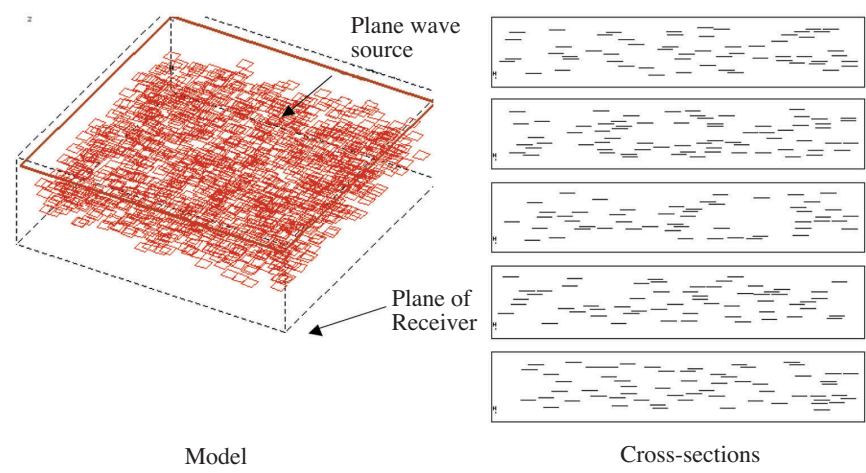


Figure 3—Example of a crack model constructed to investigate wave-speed and attenuation using plane waves showing the source and receiver planes and 2D cross-sections (from Hildyard, 2001)

Seismic wave propagation to diagnose the state of fracturing

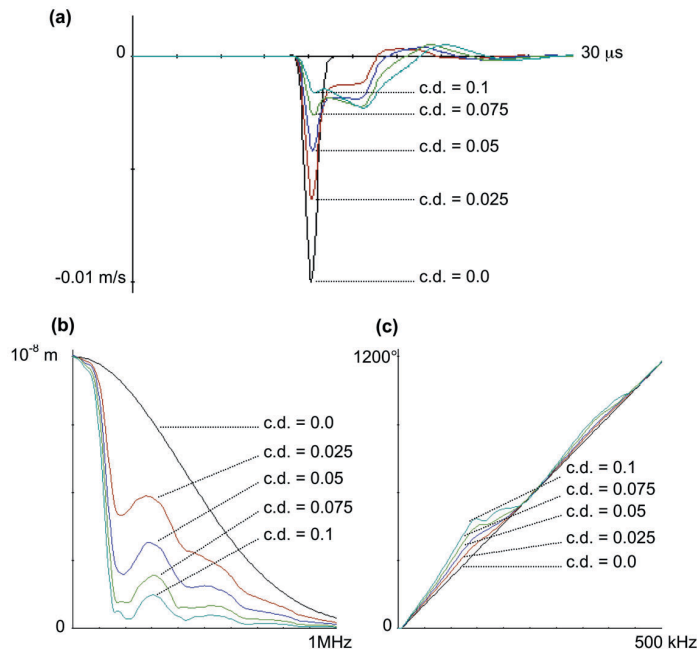


Figure 4—Waveforms recorded through crack models with crack densities ranging from 0 through to 0.1 for 11.3 mm square cracks. (a) Time-domain waveforms. (b) Fourier amplitude spectrum. (c) Fourier phase-difference relative to the input waveform. A straight line in (c) would indicate a frequency-independent velocity

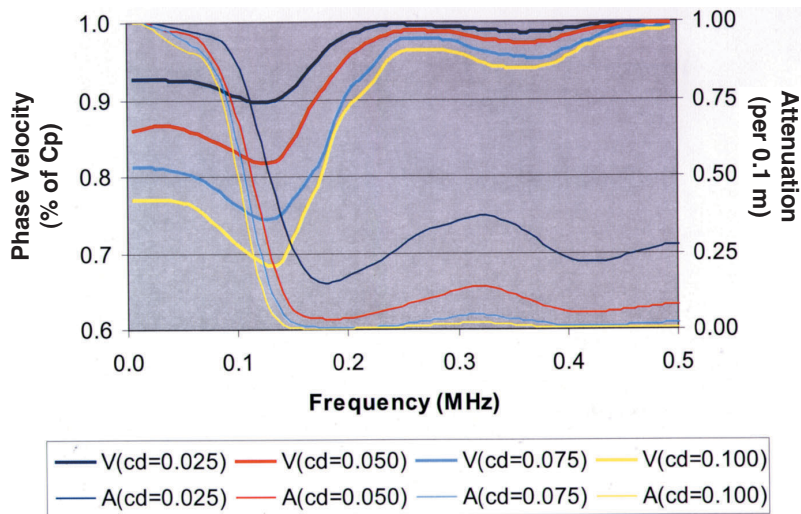


Figure 5—P-wave velocity and attenuation spectra for a distribution of 12 element (11.3 mm) open cracks with a crack density of 0.025, 0.05, 0.075 and 0.1, (from Hildyard, 2001)

Wave modelling and the 'Omnibus' project

This section covers selected results from the 'Omnibus' project, a European Union-funded project under the fifth framework EURATOM programme. The objective of this project was 'to develop tools and associated technologies for monitoring the rock barrier in both potential and operational deep underground repositories for nuclear waste disposal/storage'. The project required the development of a down-hole ultrasonic tool suitable for both hard-rock and soft-rock application, and the development of new advanced methods for processing and interpreting the data. A summary of the project and selected results are given in Pettitt *et al.* (2003).

One aspect of the project was to use wave propagation

models to improve the interpretation of ultrasonic velocity measurements, and to provide some relationship to the underlying microstructure. A series of numerical simulations were produced to model ultrasonic waves propagating through large numbers of cracks with varying crack density, crack size, fluid-filling, orientation and wave type. These simulations were based on two laboratory and two *in situ* experiments. The objective of these simulations was to provide the Omnibus project with a large theoretical data-set from models with a known microstructure, and to provide a methodology for analysing the waveforms.

The first requirement was to develop a methodology for analysing changes in wave-speed and amplitude. Previous results (Hildyard, 2001) showed that frequency-domain analysis reveals important effects not apparent in the time-

Seismic wave propagation to diagnose the state of fracturing

domain waveforms. However, the method used in Hildyard (2001) was found to be impractical for ultrasonic surveys as it requires recordings from two positions along the wave path, and because it intentionally decouples the effects of cracks from the effects of geometry. The ultrasonic waveforms obtained in experiments and measurements contain the effects of geometry, such as loss in amplitude due to geometric spreading, and reflections and converted waves from boundaries and interfaces. Since the effect of cracks cannot be isolated in these measurements, the models in this project needed to include geometric effects so that they could be directly compared with measurements from specific experiments.

In addition, the measurements do not include a measurement near the source. This means that different recordings at the same position but at a different point in time must be compared against one another. As a result, a relative method was used where waveform 1 is the chosen reference waveform, and waveform 2 is the recorded waveform at a later point in time. In this case, the change in wave-speed is related to the phase-difference by the following:

$$c_1(\omega) - c_2(\omega) \approx \frac{c_2(\omega)c_1(\omega)}{\omega(x_2 - x_1)} (\phi_2 - \phi_1) \quad [5]$$

where w is frequency, $c_1(\omega)$ and $c_2(\omega)$ are the wave-speeds and $\phi_1(\omega)$ and $\phi_2(\omega)$ the phase functions of the two waveforms, and $x_2 - x_1$ is the path-length. The above formula shows that although it is non-trivial to calculate the actual change in wave-speed, the phase-difference is directly (but not proportionally) related to this change in wave-speed. The phase-difference can therefore be used as an indicator of change in wave-speed. Similarly, the ratio of the Fourier amplitude spectra gives a measure of relative attenuation. The above is similar to methods employed by Milev *et al.* (1999). The relative method therefore entails extracting graphs of phase-difference and amplitude ratio relative to some reference received waveform. The spectral phase difference then relates to the change in wave-speed while the spectral amplitude ratio relates to change in attenuation.

This methodology was then applied to modelling the specific geometries of four experiments. The first experiment recorded ultrasonic waveforms through sandstone cubes for different block orientations and wave types and under a range of different loading conditions, using true triaxial loading to induce cracking along a single direction. The models of this experiment had the most detailed model variations, with 534 distinct models investigating the effects of variations in crack density, crack size, and fluid-filling, on P-waves and two polarizations of S-waves, for wave-paths either parallel or transverse to the cracks. The second experiment was for a uniaxial compressive test in mudstone and 55 models investigated this geometry with wave propagation through two orthogonal crack sets at different path angles. Two *in situ* experiments were performed at test sites in mudstone and granodiorite. These have the added complication that the fracture zone is only a fraction of the volume and a fraction of the path length. A series of 78 model variations investigated how the size and shape of the fracture zone will influence the waveforms for *in situ* measurements and whether such differences are sufficiently detectable. The total of 667 models required more than one year's worth of computer time—most models had more than ten million elements, and many had tens of thousands of cracks. The work was possible only through access to the supercomputing cluster ('Nessc') at Liverpool University.

Selected results from these models are shown in Figures 6 to 10. Figure 1 contains example data from the laboratory experiments on sandstone cubes under triaxial loading conditions. This showed that the wave-speed and the amplitude increased considerably as the sample was loaded, and also slowed considerably after new micro-crack generation. Figure 6 shows wave patterns from the models of some of the sandstone experiments clearly demonstrating both the delay in the wavefronts and reduction in amplitudes due to open cracks. Figure 7 comprises waveforms from a 2D model attempting to re-create the increase in wave-speed with loading, prior to crack development, as observed in the experiment in Figure 1a. This stress dependence in the waveforms was achieved through modelling a cracked

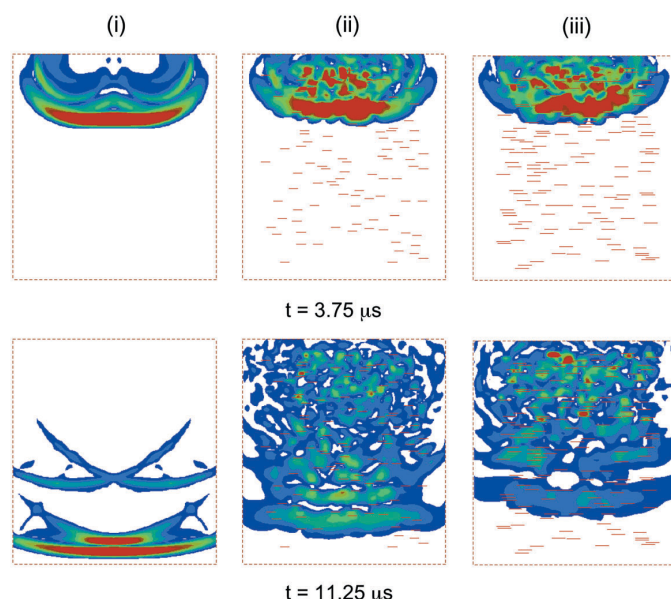


Figure 6—Models of the sandstone laboratory experiments showing wave patterns (snapshots of particle velocity) at an earlier and later time for three different crack models. (i) Elastic (ii) Crack density 0.05, crack size 2 mm (iii) crack density 0.10, crack size 3 mm

Seismic wave propagation to diagnose the state of fracturing

medium where open cracks were given a random aperture, and hence close under different load stresses. Results do show a stress dependence in the wave-speed. Figure 8 shows how the amplitudes from waveforms can be analysed in the Fourier domain and that the frequency at which attenuation occurs provides information on the size of cracks. Conversely, Figure 9 shows that changes in phase difference can provide information on the crack density. Importantly, the models demonstrated that these effects were not necessarily evident in the time-domain waveforms. Figure 10 illustrates the wave propagation in models of the *in situ* experiment showing the wave interaction with the fracture zone. Indications from these models were that changes to either the crack density, the size of the fracture zone, or the size and orientation of fractures, could be observed with sufficiently accurate recordings.

Results showed that the effects of crack density and crack size are coupled and problems were identified with inferring crack density from wave-speeds estimated simply using arrival times from the time-domain waveforms. These two effects are more readily decoupled in the frequency domain. In general, the relative Fourier amplitude should be useful for estimating crack size, while the low frequency phase-difference has a direct relationship to crack density. Geometric effects are also visible in the results, making modelling an important tool in the interpretation phase. Models with a simple approximation of fluid-filled cracks showed that if changes are observed in P-waves only, then it probably indicates a change in the fluid content of the cracks.

The use of active seismic measurements to address rock engineering problems in South African mines

Seismic monitoring is widespread on South African gold mines and more recently on the platinum mines. These provide a passive means for studying the rock mass, identifying regions of high seismicity in space and time and, through source inversion, knowledge of the types of failure occurring.

Nevertheless, active seismic measurements have to a large extent been neglected. As has been motivated in the previous sections, such measurements provide an ability to diagnose the state of the rock mass. In particular, the seismic waves have a direct mechanical interaction with both mining-

induced fractures and geological joints and so provide a means of interpreting the fracturing in the rock. Such measurements could potentially be of great benefit to rock engineers, as knowledge of the fracturing in pillars and in rock surrounding stopes and tunnels, has important implications for rock engineering design and safety.

Through current parliamentary-funded projects, CSIR-Miningtek is taking the initial steps to evaluate the use and benefits of active seismic velocity surveys in the South African mining industry. One approach would be to use ultrasonic tools being developed for use in nuclear waste depositories, such as the micro-velocity probe (Maxwell *et al.*, 1998). This probe is used to log the variation in wave-speed along a borehole using ultrasonic sensors spaced up to 30 cm apart. It could for example be used to log the changes in velocity in the fracture zone of stopes, determining the degree of fracturing and the distance over which the fracture zone extends into the hangingwall. The initial approach being pursued at Miningtek, however, will be to examine how successfully existing, in-house, low frequency seismic monitoring tools can be applied, before investigating these other techniques.

One important application for these techniques would be to develop a method to determine the degree or extent of fracturing in pillars. One case very relevant to platinum mines is being able to determine whether a 'crush' pillar has failed correctly. Crush pillars are small pillars intended to fail while close to the face. Incorrect design of these pillars can mean that the core of the pillar remains intact and fails more violently at a later stage when the mining face is well ahead of the pillar.

Numerical models were constructed to determine whether this could feasibly be investigated using in-house, low frequency, seismic monitoring equipment (viz. the Ground Motion Monitor developed at CSIR). This device applies high frequency filtering from 2 kHz, and model assumptions were therefore a hammer-type source generating frequencies around 2 kHz. Figure 11 shows the model geometry for a 6 m by 3 m pillar, with a source and receiver investigating a 3 m path through the centre of the pillar. Four models investigated different sizes of the fracture zone—an unfractured elastic pillar and pillars with a fractured 'annulus' of 0.4 m, 0.85 m and 1.3 m—this last case being

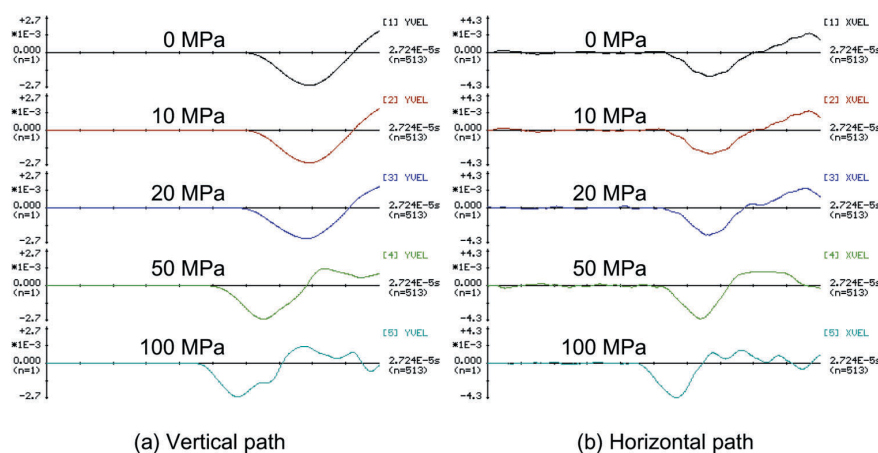


Figure 7 Waveforms from 2D models attempting to capture the stress-dependence of wave-speed for vertical and horizontal paths at different hydrostatic loading states. The model had a crack density of 0.4, with both horizontal and vertical cracks ranging in length from 2 mm to 5 mm, and with 'apertures' ranging from 4 to 40 μm

Seismic wave propagation to diagnose the state of fracturing

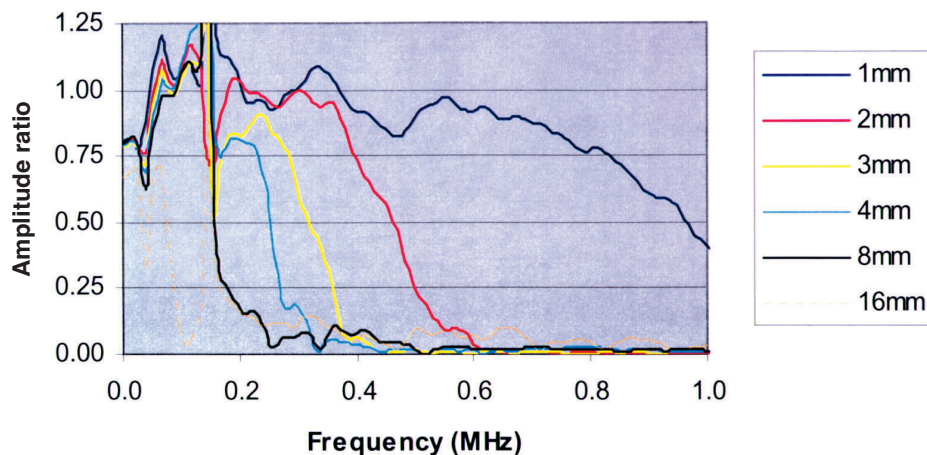


Figure 8—Fourier amplitude ratio relative to an uncracked model for P-wave propagation transverse to cracks of increasing size, maintaining a crack density of 0.05

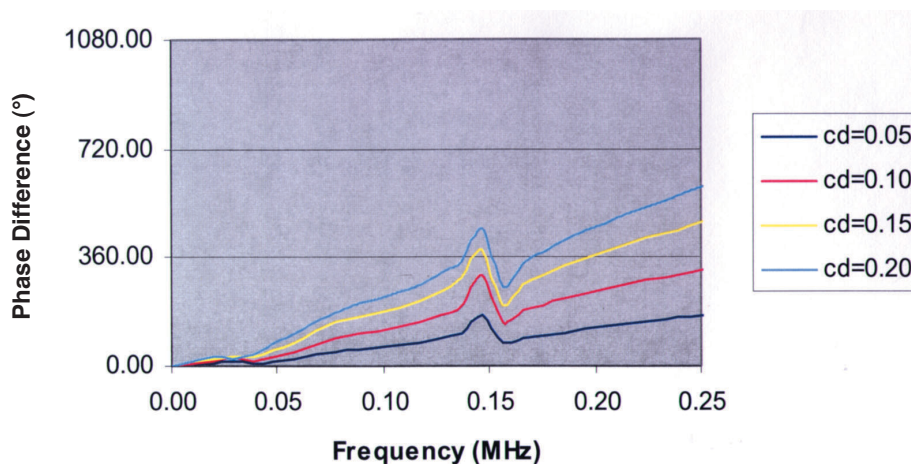


Figure 9—Fourier phase-difference relative to an uncracked model for P-wave propagation transverse to cracks with increasing crack density and a constant crack size of 2 mm

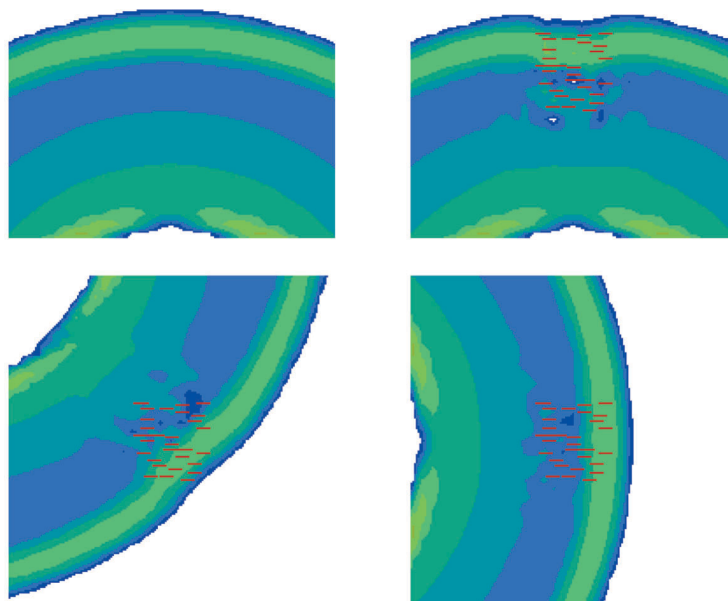


Figure 10—Wave propagation in models of the *in situ* experiment in diorite showing interaction with the fracture zone, contrasted for the elastic model and three source orientations for cracked models with 6 cm cracks and crack density of 0.05

Seismic wave propagation to diagnose the state of fracturing

almost fully fractured. In all cases the fractures ranged in size from 0.2 m to 0.6 m with a crack density of 0.1. Figure 12a shows the effect of the fracturing on the time domain waveforms. Clear differences in the arrival times can be observed as the fractured region is increased. Figure 12b shows that the effects on Fourier phase difference are unambiguous, and that the techniques mentioned above would be useful in such analysis. The primary effect of these sorts of fracture sizes and frequencies are on wave-speed. Higher frequency investigations would allow the attenuation effects also to be studied, potentially improving both the time-domain and frequency-domain interpretations.

A second important mining application is in the investigation of jointing and fracturing in the hangingwall of stopes, which is of obvious significance for evaluating support requirements. Figure 13 shows a cross-section through a model constructed to evaluate simple attempts to measure velocity in this fracture zone. The hangingwall of the stope was assumed to have two parting planes with the initial 1.25 m of the fracture zone having a crack density of 0.2 and the next 1.25 m a crack density of 0.1. Again, based on the equipment likely to be used in initial experiments, the assumptions were a hammer-type source with vertical impact generating frequencies around 2 kHz. Receivers were spaced at 2 m intervals from the source and recorded vertical motion.

Receiver waveforms are shown in Figure 14 for a fractured and unfractured hangingwall, along with the theoretical P-wave, S-wave and Rayleigh wave arrival times for an unfractured material (5740 m/s, 3510 m/s and 3170 m/s respectively). The P-waves in this test are clearly

swamped by the shear and Rayleigh waves, and care will need to be taken in such measurements not to choose the P-wave arrival much later than its true arrival, and hence infer a much greater degree of fracturing. Figure 15 shows these same waveforms zoomed tenfold. The arrival times for the unfractured model are consistent with theory. The P wave-speed in the fractured model is slowed by approximately 18%. The model identifies a second problem to be aware of for this geometry before such measurements are naively interpreted. The arrival at 14 m is earlier than would be expected. The waves can travel through the highly fractured region into faster regions and then back through the fractured region to the receiver. At some distance the average wave-speed for such a path is faster than the direct path. For this geometry, measurements at 14 m and beyond will underestimate the wave-speed and hence underestimate the degree of fracturing. The above behaviour is well-understood in standard refraction surveys and is used to yield the depth of layers. However, correct interpretation of results will require an appropriate density of the receivers.

The above numerical examples have demonstrated possible applications in mining, where making active seismic velocity measurements could be of benefit in providing rock engineers with an indication of fracturing. Higher frequency approaches should also be examined, as the attenuation of waves will provide further information. Naively applying such techniques can, however, be misleading and theoretical and numerical models should be used to help develop the applications.

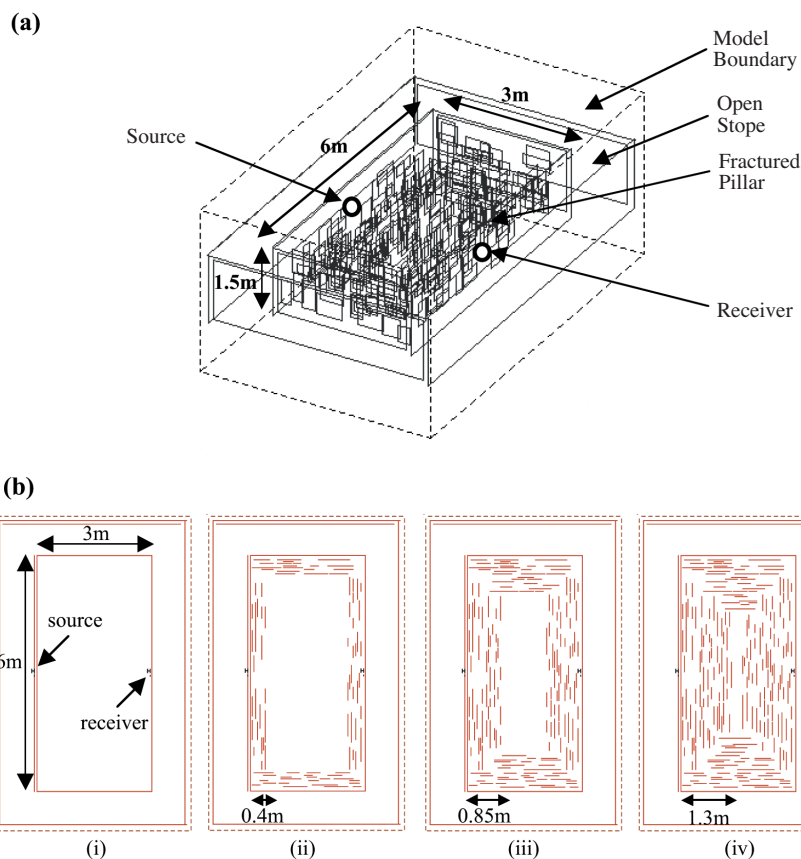


Figure 11—Geometry for the fractured pillar models. (a) Three-dimensional view of fractured pillar showing positions of source and receiver and dimensions. (b) Plan cross-sections through four pillar models with different sized regions of fracturing with fractured 'annulus' varying from (i) 0 m (elastic) (ii) 0.4 m (iii) 0.85 m (iv) 1.3 m. In all cases the fractures range in size from 0.2 m to 0.6 m with a crack density of 0.1

Seismic wave propagation to diagnose the state of fracturing

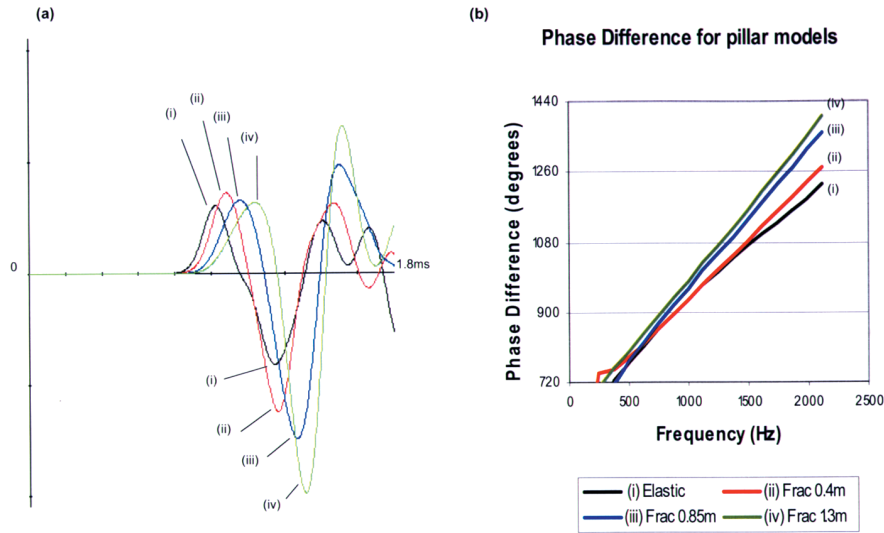


Figure 12—Results for the four pillar models showing the effect of different sizes of the fractured region on wave-speed. (a) Time-domain waveforms (b) Fourier phase-difference relative to the source waveform. (i), (ii), (iii) and (iv) refer to the four models in Figure 11b

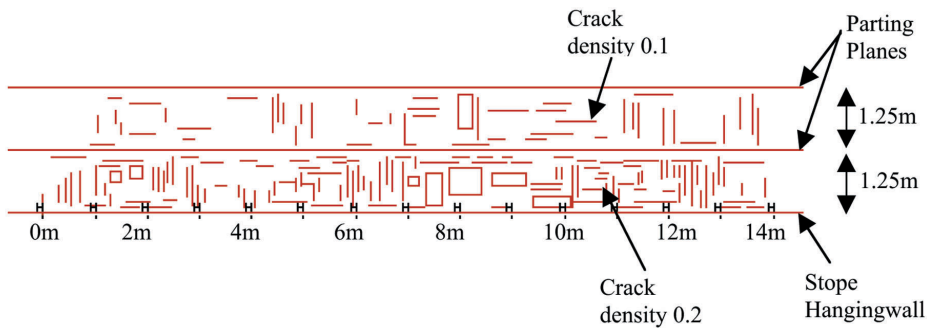


Figure 13—Cross-section through the three-dimensional fractured hangingwall model

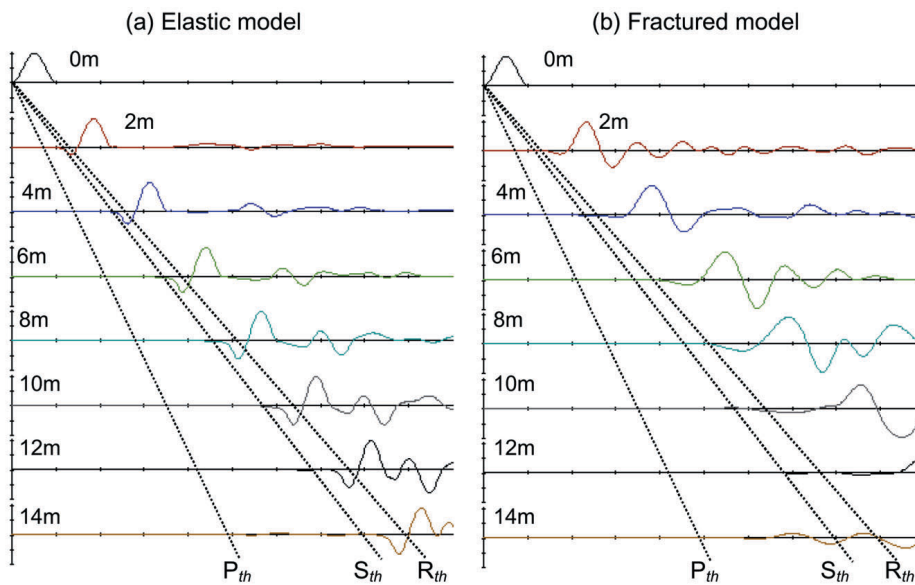


Figure 14—Waveforms received in the hangingwall at 0 m, 2 m, 4 m, 6 m, 8 m, 10 m, 12 m and 14 m from the source, with a time window of 5 ms. P_{th} , S_{th} and R_{th} are the theoretical arrival times for the P, S and Rayleigh waves. Amplitudes aren't shown but are scaled according the peak in each trace and reduce with increasing distance

Seismic wave propagation to diagnose the state of fracturing

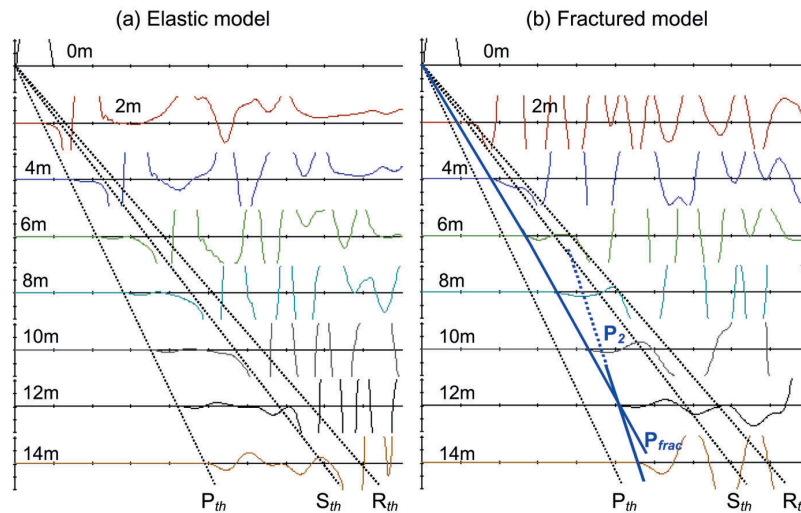


Figure 15—Waveforms as for Figure 14, but with amplitudes zoomed tenfold. P_{th} , S_{th} and R_{th} are the theoretical arrival times for the P, S and Rayleigh waves. P_{frac} is the P-wave arrival for the fractured model, while P_2 is a second P-wave arrival which after a certain distance arrives before the direct wave

Conclusions

This paper has given examples of how active seismic measurements can be used to diagnose fracturing. Many of the examples and techniques have been developed for ultrasonic measurements at nuclear waste repositories, but the same techniques can be applied to more highly fractured rock surrounding mine openings.

- Experiments and models show clear changes in the arrival times and amplitude of waves due to different degrees of fracturing
- The effects of crack density and crack size are coupled, and results indicate that these effects are more readily decoupled in the frequency domain
- Methods were proposed for analysing these changes in the Fourier domain. In general, the Fourier amplitude should be useful for estimating crack size, while the low frequency phase-difference has a direct relationship to crack density
- Measurements are geometry-dependent in that the waveforms include effects due to both cracks and the geometry. Naive interpretations can be misleading and theoretical and numerical models should therefore be used in the interpretation of results from such measurements
- Numerical examples were used to demonstrate that active seismic measurements could be of benefit to addressing rock engineering problems experienced in South African mines—in particular to help determine whether pillars have crushed and to determine the degree of fracturing in the hangingwall of stopes.

Acknowledgements

The Omnibus project is co-funded by the EU, as part of the fifth framework Euratom programme. It consists of four partners: Liverpool University and Applied Seismology consultants in the UK, and INERIS and ANDRA in France. Work presented from Hildyard, (2001), was largely conducted under GAP601b, a project sponsored by SIMRAC (Safety in Mining Research Advisory Council). Models relating to applications in South African mines were

performed under a parliamentary-funded CSIR-Miningtek project, investigating blocky hangingwall behaviour.

References

1. O'CONNELL, R.J. and BUDIANSKY, B. Seismic velocities in dry and saturated cracked solids. *J. Geophys. Res.*, vol. 79, 1974. pp. 5412–5426.
2. CRAMPIN, S. A review of wave motion in anisotropic and cracked elastic-media. *Wave Motion*, vol. 3, 1981. pp. 343–391.
3. HUDSON, J.A. Wave speeds and attenuation of elastic waves in material containing cracks. *Geophysical Journal R. Astr. Soc.*, vol. 64, 1981. pp. 133–150.
4. GIBOWICZ, S.J. and KIJKO, A. *In An introduction to mining seismology*, International Geophysics series, Publ. Academic Press, vol. 55, pp. 111–115.
5. YOUNG, R.P. and MAXWELL, S.C. Seismic characterization of a highly stress rock mass using tomographic imaging and induced seismicity. *J. of Geophys. Res.*, vol. 97, no. B9, August 1992. pp. 12361–12373.
6. MAXWELL, S.C. and YOUNG, R.P. Seismic imaging of rock mass responses to excavation. *Int. J. Rock Mech. Min. Sci.*, vol. 33, no. 7, 1996. pp. 713–724.
7. CARLSON, S.R. and YOUNG, R.P. Acoustic emission and ultrasonic velocity study of excavation-induced microcrack damage at the underground research laboratory. *Int. J. of Rock Mech.*, vol. 30 (7), 1993. pp. 901–907.
8. COLLINS, D.S. Excavation induced seismicity in granitic rock - a case study at the Underground Research Laboratory, Canada. PhD Thesis, Keele University, UK, 1997. pp. 1–256.
9. YOUNG, R.P. and COLLINS, D.S. Seismic studies of rock fracture at the underground research laboratory Canada. *Int. J. Rock Mech. Min. Sci.*, special issue on geophysics in rock mechanics, vol. 38, 2001. pp. 787–799.
10. PETTITT, W.S., BAKER, C., YOUNG, R.P., DAHLSTRÖM, L.-O., and RAMQVIST, G. The assessment of damage around critical engineering structures using induced seismicity and ultrasonic techniques. *Pure Appl. Geophys.*, 159, 2001. pp. 179–195
11. BAKER, C. and PETTITT, W. Laboratory tests to investigate the static and dynamic moduli of Crosland Hill sandstone, in SAFETI Mid-term Progress Report, Applied Seismology Consultants Ltd., UK. 2003.
12. HILDYARD, M.W. 'Wave interaction with underground openings in fractured rock', PhD Thesis, University of Liverpool, 2001, pp. 283.
13. PETTITT, W.S., COLLINS, D.S., HILDYARD, M.W., YOUNG, R.P., BALLAND, C., and BIGARRE, P. An ultrasonic tool for examining the excavation damaged zone around radioactive waste repositories—the OMNIBUS project. Eurad04. 2003.
14. MILEV, A.M., SPOTTISWOODE, S.M., and STEWART, R.D. Dynamic response of the rock surrounding deep level mining excavations. *9th Intl. Congress on Rock Mechanics*, Paris, France. 1999.
15. MAXWELL S.C., YOUNG, R.P., and READ, R.S. A micro-velocity tool to assess the excavation damaged zone. *Int. J. Rock Mech. Min. Sci.*, vol. 35, 1998. pp. 235–247. ◆